Tunneling spectroscopy of disordered two-dimensional electron gas in the quantum Hall regime

Gilad Barak,[1] Amir Yacoby,[1] and Yigal Meir[2]

[1]*Department of Physics, Harvard University, Cambridge, Massachusetts 02138, USA*
[2]*Department of Physics, Ben Gurion University, Beer Sheva 84105, Israel*

The tunneling density of states (TDOS) into a disordered two-dimensional electron gas is calculated in the quantum Hall regime, including electron-electron interactions. Combining general arguments and a detailed Hartree-Fock calculation, it is demonstrated that the quenching of the kinetic energy by the applied magnetic field leads to several universal features, nearly independent of the disorder potential, corresponding to the addition and removal spectrum in the valleys and tips of the disorder potential. These features are manifested as "sashes" in the TDOS spectra, and are in quantitative agreement with recent measurements. It is predicted that more such features will become observable with decreasing potential fluctuations.

The quantum Hall effect (QHE) has been at the forefront of science in the past three decades,[1,2] as the interplay between high magnetic field, disorder, and electron-electron (*e-e*) interactions led to a plethora of unique phenomena, in particular, different types of fractionally charged, possibly non-Abelian quasiparticles.[3,4] As there is great interest in the experimental search for such elementary excitations, it is imperative to understand which of the experimental observations indeed indicate such unique physics, and which can be explain by more mundane physics. In this spirit we analyze in detail recent measurements of the tunneling density of states (TDOS) into the bulk of a QHE system, which were reported by Dial *et al.*[5] using time domain capacitance spectroscopy.[6] These measurements revealed a set of TDOS features ("sashes"), comprising high-energy bands, whose bottom decreases linearly with density. These observations led to some excitement, as one of the suggested explanations of these features involved alternate types of excitations in the quantum Hall regime. The ramifications of such yet unseen excitations on the physics of the QHE may be far reaching. However, we present here a possible mechanism that quantitatively reproduces these observations based on standard quantum Hall physics in the presence of *e-e* interactions without invoking any such mechanism. Moreover, this mechanism demonstrates that these features are nearly universal, independent of the details of the disorder potential.

Three energy scales determine the measured spectrum: the cyclotron energy $\hbar\omega_C$, the disorder potential fluctuations $\Delta V_{\text{disorder}}$, and the Coulomb interaction between electrons, characterized by $e^2/\varepsilon l_B$. Here $\omega_C = eB/m^*$, e the electron charge, B the applied magnetic field, m^* the effective mass, ε the sample dielectric constant, and $l_B = \sqrt{\hbar/eB}$ the magnetic length (with $\hbar = h/2\pi$, h being Planck's constant). The picture described below is valid under strong magnetic fields, and assumes $e^2/\varepsilon l_B, \Delta V_{\text{disorder}} < \hbar\omega_C$. The electron density is described by the filling factor $\nu = BA/\phi_0$, where A is the sample area and $\phi_0 = hc/e$ is the quantum flux (c is the velocity of light). In addition to the magnetic length, there are two other length scales, the distance l_G to the metallic gate (from which the electron tunnel), and the thickness d of the two-dimensional electron gas (2DEG). l_G screens the *e-e* interactions and the potential fluctuations, thus leading to the fact that electrons localized at different dips of the disorder potential are only weakly interacting, while the interaction between electrons within the same potential dip is practically unscreened. Thus, for small ν the effective Hamiltonian for the system is given by

$$H = \sum_{D \in \text{valleys}} \sum_{\sigma,\sigma',m,m'} \left(V_D^m n_{m,\sigma}^D + V_C^{m,m'} c_{m',\sigma'}^D{}^\perp c_{m,\sigma}^D{}^\perp c_{m',\sigma'}^D c_{m,\sigma}^D \right) \\ + \sum_{\text{Extended}} V_E n^E. \tag{1}$$

The first sum considers separately local minima in the disorder potential, and the sum over m and m' are over the eigenstates of each such potential dip (here, $c_{m,\sigma}^D{}^\perp$, $c_{m,\sigma}^D$, and $n_{m,\sigma}^D$ are the creation, annihilation, and number operators for these states, respectively). The energy associated with occupying such states arises from the local disorder potential V_D^m, and the Coulomb interaction $V_C^{mm'}$ with other electrons occupying the same valley. We expect the lowest-energy wave functions to span an area of $\sim l_B^2$ and hence $V_C^{00} \sim e^2/\varepsilon l_B$, up to a correction due to the finite thickness d. The last term in (1) corresponds to extended states, not localized by a specific disorder well, and giving rise to a continuous energy spectrum.

Following the convention used in Ref. 5, where the Fermi level E_F is set to $E = 0$, unoccupied states give rise to an $E > 0$ band, corresponding to adding electrons to the empty, disorder-broadened Landau level [I in Fig. 1(a)]. This band will persist for higher filling factors, but the top of the band will decrease linearly, as E_F rises with ν. Two additional features will become relevant for the TDOS with increasing ν: Removing an electron from an occupied state gives rise to an $E < 0$ band [II in Fig. 1(a)], and adding a second electron (of opposite spin) to an occupied state, with the cost of an additional Coulomb energy V_C^{00}, effectively creates a "second Hubbard band" [H1 in Fig. 1(a)]. Since V_C^{00} is independent of density for high magnetic fields, the high-energy band should replicate the band of occupied states, shifted by the constant energy V_C^{00}.

As ν increases, the bottom of the higher Hubbard band should extrapolate to zero at $\nu = 1$, since there all the single-particle states are occupied and the Fermi energy lies at the bottom of the second Hubbard band. The whole TDOS structure for $\nu < 1$ is reflected about the $E = 0$ axis for $\nu > 1$
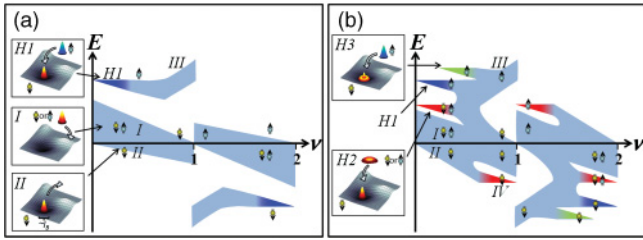
FIG. 1. (Color) (a) Schematic of the TDOS dependence on the filling factor. For $\nu = 1$, the TDOS comprises a disorder-broadened band (I). Energies are defined with respect to the chemical potential. For small filling factors, populated states (II) comprise electrons sitting at the ground state of disorder wells. Under strong magnetic field, the wave functions of the lowest-energy states in a disorder potential well are only weakly dependent on details of the disorder potential. A second Hubbard band is created (H1), resulting from the strong Coulomb interaction of adding an opposite-spin electron to an occupied state. Arrows indicate spin orientation. (b) Schematic of the TDOS dependence on the filling factor, including secondary bands arising from interactions with higher angular momentum eigenstates. In addition to the high-energy band H1, a lower band (H2) arises from the injection of an electron into the more extended, higher-energy eigenstate. A higher-energy band (H3) is expected for larger filling factors, corresponding to the addition of an electron to a disorder potential valley already occupied by two particles.

due to particle-hole symmetry. We identify the entire gap to the second Hubbard band as the "$\nu = 1$ sash" reported in Ref. 5.

In principle, this description should be augmented by the physics of exchange and correlations which become relevant as ν increases. Close to $\nu = 1$ a strong exchange gap[7–9] arises between the two spin types [III in Fig. 1(a)]. The energy to add a neighboring same-spin electron becomes lower, leading to an abrupt upshift of the TDOS of the minority spins. We claim that the ingredients described above and modeled in detail below are enough to understand the experimental observations, indicating that electronic correlations, leading, for example, to the fractional quantum Hall effect, are not necessary to explain the experiment. An additional feature observed in the tunneling measurements is a gap near $E = 0$. This gap arises from effective impedance to the tunneling, due to the required redistribution of charge in the system in order to allow for the

injection of an electron.[10–12] This effect is well understood, and will not be modeled here.

A quantitative estimate of the characteristic gap to the second Hubbard band V_C^{00} can be obtained by assuming a specific form for the ground state in a specific valley. Assuming, for simplicity, radial symmetry near the bottom of the valley, the Hartree energy between the two spins occupying this state, for a 2DEG well width of 23 nm (Ref. 5) is $V_C^{00} \approx 3.5$ meV for $B = 4$ T, in excellent agreement with the measurements.[5] Furthermore, this energy gap scales as $B^{1/2}$, in agreement with the reported observation.

Additional lower-energy bands may be created, arising from the injection of electrons into higher-energy states in the well [H2 in Fig. 1(b), and $m' > 0$ in Eq. (1)]. Experimental observation of such features requires that the energy cost associated with this tunneling process be larger than the disorder broadening. Importantly, the short distance between the tunneling electrode and the 2DEG (Ref. 5) acts to lower the interaction energy with higher-energy states, as these are spatially more extended [see the inset to Fig. 1(b)]. Calculating the Coulomb interaction between two electrons occupying the two lowest-energy states gives $V_C^{01} \approx 2$ meV at 4 T and $V_C^{01} \approx 2.8$ meV at 8 T, again in excellent agreement with the measured feature termed the "^{2}CF sash" in Ref. 5. The exchange interaction between different eigenstates is very weak, so that in the limit of small filling factors no discernable separation is expected between the secondary bands arising from different spins. An important attribute of the V_C^{01} gap is its symmetry at approximately $\nu = 1/2$ [IV in Fig. 1(b)], reflecting the electron-hole symmetry in the majority-spin band. Again, this property is observed in the measurements[5] ("$\nu = 1/2$ sash"). In addition to the low-energy bands, higher-energy features can emerge, in principle, which correspond to the addition spectrum of an electron to a location that is already doubly occupied [H3 in Fig. 1(b)]. These features are not observed in the measurements, probably due to their stronger dependence on the local disorder potential profile, smearing them beyond the experimental resolution limit.

The actual calculation of the TDOS into a two-dimensional system in the presence of strong magnetic field, disorder, and e-e interactions is numerically challenging. Here we present a restricted Hartree-Fock calculation of the TDOS into a quasi-one-dimensional system, and demonstrate that it is sufficient to reproduce the physics described above, when the
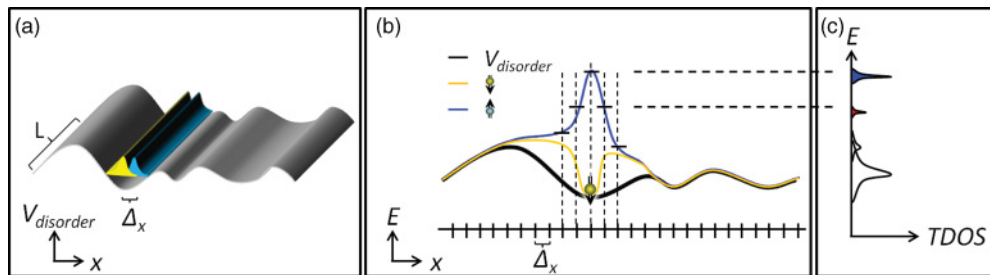

FIG. 2. (Color) (a) The Hartree-Fock model employed to study the influence of Coulomb interactions on the tunneling density of states. (b) The background disorder potential (black line) gives rise to a broad tunneling density of states. When an electron occupies a potential valley, the resulting Coulomb interaction creates high-energy bands for additional occupation of the same site with an opposite spin electron, as well as occupation of nearby sites. (c) The resulting tunneling density of states is comprised of the low-energy disorder-broadened band, and several high-energy bands corresponding to the discrete energies to occupy neighboring states of an occupied site.
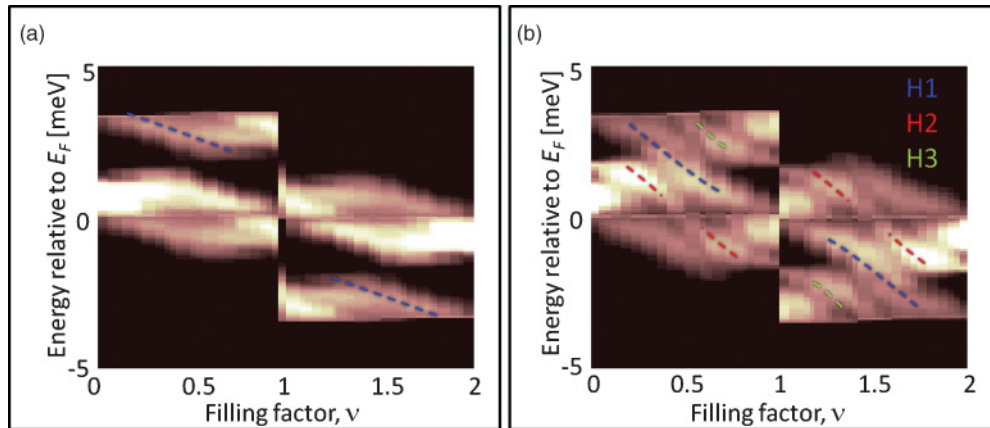
FIG. 3. (Color) (a) A Hartree-Fock calculation of the TDOS, when the screening length is comparable to the magnetic length ($l_{sc} \approx l_B$). White features correspond to high TDOS. The strong feature marked by the dashed blue line is a "second Hubbard band" created due to the added energy required to inject a particle into a disorder well already occupied by an opposite spin particle. (b) Calculated TDOS when the screening length is larger than the magnetic length ($l_{sc} \approx 4l_B$). Additional high-energy features arise due to interactions between neighboring states (see the text).

width of the wire L corresponds to the quantum confinement of the wave function in the two-dimensional system ($L \sim 50$ nm). Due to the quenching of the kinetic energy, the Hamiltonian contains only two terms, the disorder potential and the exponentially screened Coulomb interactions. The calculation is limited to states in the lowest Landau level, and the electronic wave functions are assumed to be eigenstates of the disorder-free Hamiltonian (in the Landau gauge). Disorder is introduced in the model by randomly determining a background potential profile. Calculations involve averaging over many (several thousands) such potential instances, so as to avoid any disorder-specific effects. The model assumes periodic boundary conditions in the transverse direction, quantizing the separation between neighboring states to $\Delta_x = \phi_0/BL$ [Figs. 2(a) and 2(b)]. Since the wave functions are not calculated self-consistently, this approximation effectively assumes that the disorder profile varies only in one direction. The role of higher-energy eigenstates is played by farther-away neighbors, giving rise to lower-energy bands similarly to the qualitative description [see Figs. 2(b) and 2(c)].

The TDOS is given by the tunneling current

$$I(V) \propto \int [f(\varepsilon - eV) - f(\varepsilon)]\nu_{2DEG}(\varepsilon; T)\nu_M(\varepsilon)d\varepsilon, \quad (2)$$

where $\nu_{2DEG}(\varepsilon;T)$ and $\nu_M(\varepsilon)$ are the density of states in the probed 2DEG and in the metallic electrode, respectively, $f(\varepsilon)$ is the Fermi function, and V is the bias applied between the metallic electrode and the 2DEG. We assume, for simplicity, that the density of states in the metallic electrode is independent of energy, while that of the 2DEG, as mentioned below, may depend on temperature, due to the interactions. Figure 3 presents the results of the calculation. In Fig. 3(a), the screening length is assumed equal to the magnetic length, strongly attenuating the Coulomb interactions between states at different sites and reproducing the first Hubbard band alone (dashed blue line). For longer screening lengths [$4l_B$ in Fig. 3(b)], two additional features are observed, corresponding to the described bands H2 and H3. Additional features resulting

from considering farther-away occupied sites are attenuated by screening and disorder.

An important ingredient in the reported experimental results[5] is a strong temperature dependence of the high-energy
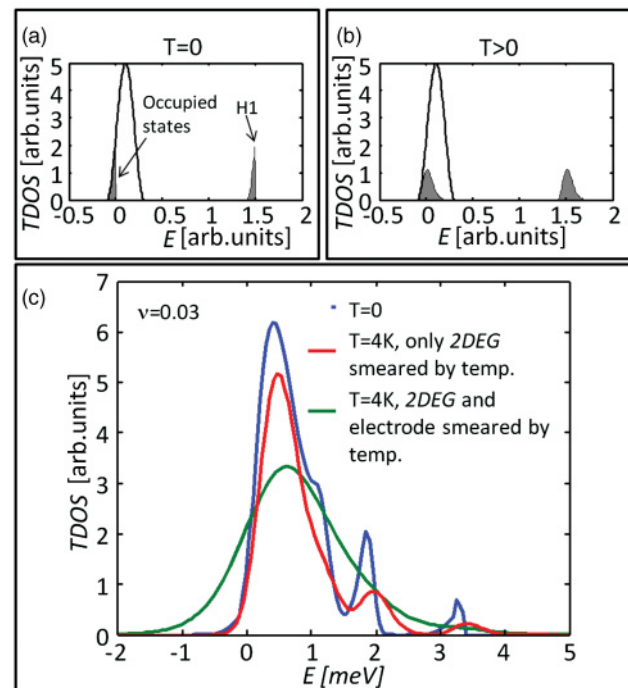

FIG. 4. (Color) (a), (b) Simplified model for the 2DEG density of states, presenting the nontrivial influence of temperature. (a) For $T = 0$, all states below the Fermi level (set here to $E = 0$) are occupied, giving rise to a duplicate high-energy band H1. (b) For $T0$, occupation of the low-energy states is broadened. The high-energy second Hubbard band duplicates this broadening. (c) The calculated TDOS at $T = 0$ (blue) for low filling factor of $\nu = 0.03$. A temperature increase to 4 K smears the TDOS structure, but the characteristic structure is still observable (red). Considering, in addition, the influence of the heated charge distribution in the tunneling electrode renders this structure undistinguishable (green).

features that are shown to vanish for temperatures significantly smaller than the energy gap V_C^{00}. Our model reproduces this strong temperature dependence: besides the trivial broadening of the Fermi function in the metal gate, temperature also affects the occupation of states in the 2DEG. Since the high-energy features (the higher Hubbard band) depends on these occupations, they will be sensitive to small temperature variations.

Thus, temperature influences the observed signal in two ways: First, because of the Fermi function population, the occupations of the 2DEG and the metallic electrode are modified from a sharp profile in which all states below the Fermi energy are populated and no states above it are [Fig. 4(a)] to a smooth occupation distribution [Fig. 4(b)]. Second, since the TDOS of the second Hubbard band directly mirrors the occupied state distribution, it will be similarly broadened. Note that this smearing of the high-energy band is *independent* of the energy gap V_C^{00}. While the high-energy bands remain distinguishable when considering the temperature smearing arising from each of these mechanisms alone, their combined effect leads to the complete vanishing of these features.

Including temperature into the calculation, we indeed find that the high-energy features are strongly smeared [red line in Fig. 4(c)]. Allowing, in addition, for the temperature smearing of the metallic electrode we find the high-energy structure becomes completely indiscernible [green line in Fig. 4(c)], reproducing the reported observations.[5] While this model should be used with caution, due to its quasi-one-dimensional nature, the qualitative and quantitative agreement with the picture presented earlier and the experiment is encouraging, and demonstrates that fractional-QHE physics, resulting from electronic correlations, is not necessary to understand these particular features.

Recently an alternative possible explanation for Ref. 5 was given by MacDonald.[13] There, the appearance of high-energy sashes in the TDOS is explained based on correlation physics. Similarly to our analysis, Macdonald considers the low-density limit, and shows there is an energy gap when adding a same-spin electron to a region already occupied by an electron. The energy gap is explained in terms of the different correlation energies of the possible ground states of two same-spin and two opposite-spin electrons. Due to the complexity of the model, the mathematical analysis of the resulting energy gap is far more thorough in Ref. 13 than in our description here, and shows the gap can be described in terms of Haldane pseudopotentials. However, we believe the simple picture presented above provides a consistent description of all experimental observations without requiring such an elaborate formalism and specific mechanism.

To conclude, we have demonstrated that standard quantum Hall physics in the presence of interactions can explain the features observed in the experiment, demonstrating the caution one has to employ in interpreting experimental data by more exotic physics.

---

[1] T. Chakraborty and P. Pietilainen, *The Quantum Hall Effects-Fractional and Integer*, Springer Series in Solid-State Sciences No. 85 (Springer, Berlin, 1995).

[2] J. Jain, *Composite Fermions* (Cambridge University Press, Cambridge, UK, 2007).

[3] G. Moore and N. Read, Nucl. Phys. B **360**, 362 (1991).

[4] C. Nayak, S. Simon, A. Stern, M. Freedman, and S. Das Sarma, Rev. Mod. Phys. **80**, 1083 (2008).

[5] O. E. Dial, R. C. Ashoori, L. N. Pfeiffer, and K. W. West, Nature (London) **464**, 566 (2010).

[6] O. E. Dial, R. C. Ashoori, L. N. Pfeiffer, and K. W. West, Nature (London) **448**, 176 (2007).

[7] J. F. Janak, Phys. Rev. **178**, 1416 (1969).

[8] T. Ando and Y. Uemura, J. Phys. Soc. Jpn. **37**, 1044 (1974).

[9] R. J. Nicholas, R. J. Haug, K. v. Klitzing, and G. Weimann, Phys. Rev. B **37**, 1294 (1988).

[10] S. He, P. M. Platzman, and B. I. Halperin, Phys. Rev, Lett. **71**, 777 (1993).

[11] F. G. Pikus and A. L. Efros, Phys. Rev. B **51**, 16871 (1995).

[12] S. Levitov and A. V. Shytov, JETP Lett. **66**, 214 (1997).

[13] A. H. MacDonald, Phys. Rev. Lett. **105**, 206801 (2010).